Published in final edited form as:
Circ Res. 2011 January 7; 108(1): 70–84. doi:10.1161/CIRCRESAHA.110.223578.

Integrative Systems Models of Cardiac Excitation Contraction Coupling

Joseph L. Greenstein and **Raimond L. Winslow**
Institute for Computational Medicine, Center for Cardiovascular Bioinformatics and Modeling, and Whitaker Biomedical Engineering Institute, The Johns Hopkins University, Baltimore, MD, USA

Abstract

Excitation-contraction coupling in the cardiac myocyte is mediated by a number of highly integrated mechanisms of intracellular Ca^{2+} transport. The complexity and integrative nature of heart cell electrophysiology and Ca^{2+}-cycling has led to an evolution of computational models that have played a crucial role in shaping our understanding of heart function. An important emerging theme in systems biology is that the detailed nature of local signaling events, such as those that occur in the cardiac dyad, have important consequences at higher biological scales. Multi-scale modeling techniques have revealed many mechanistic links between micro-scale events, such as Ca^{2+} binding to a channel protein, and macro-scale phenomena, such as excitation-contraction coupling gain. Here we review experimentally based multi-scale computational models of excitation-contraction coupling and the insights that have been gained through their application.

Keywords

cardiac myocyte; excitation-contraction coupling; Ca^{2+}-induced Ca^{2+} release; multi-scale modeling; computational modeling

Overview of cardiac excitation-contraction coupling

Intracellular calcium (Ca^{2+}) concentration plays a number of important regulatory roles in the cardiac myocyte. These include excitation-contraction coupling (ECC)[1], intracellular signaling[2], regulation of mitochondrial function[3], gene expression[4], and cell death[2, 5]. This review article is focused on the role of Ca^{2+} in ECC in cardiac ventricular myocytes. In particular, we will review experimentally based computational models of ECC, with a specific focus on mechanisms of Ca^{2+}-induced Ca^{2+} release (CICR), and the insights that have been gained through application of these models.

The nature of ECC is linked closely to both the micro-anatomical structure of the cell, and to the arrangement of contractile proteins within the cell. The basic unit of contraction in the cardiac myocyte is the sarcomere. Individual sarcomeres are bounded on both ends by the t-tubular system[1, 6, 7]. The t-tubules are cylindrical invaginations of the sarcolemma that extend deep into the cell and approach an organelle known as the sarcoplasmic reticulum (SR). The SR is a luminal organelle located throughout the interior of the cell, and it is involved in the uptake, sequestration and release of Ca^{2+}. SR can be divided into three main

Corresponding Author: Raimond L. Winslow, PhD, Rm 315 CSEB, 3400 N. Charles St., Baltimore MD 21218, 410.516.5417 (Office), 410.516.5294 (FAX), rwinslow@jhu.edu.

Disclosures
None.

components known as junctional SR (JSR), corbular SR, and network SR (NSR). The JSR is that portion of the SR most closely approximating (within 12–15 nm)[8] the t-tubules. The close proximity of these two structures forms a micro-domain known as the dyad.

Ca^{2+}-sensitive Ca^{2+}-release channels known as ryanodine receptors (RyRs) are preferentially located in the dyadic region of the JSR membrane. In addition, sarcolemmal voltage-gated L-type Ca^{2+} channels (LCCs) are preferentially located within the dyadic region of the t-tubules, where they are in close opposition to the RyRs. Early data from freeze fracture electron micrographs suggested that RyRs are arranged in a somewhat regular lattice[9]. The assumption that RyRs are tightly packed in dyadic junctions led to estimates of 100–300 RyRs per dyad[8]. However, more recent imaging studies have demonstrated that dyadic clefts are small, where junctions contain an average of 14 RyRs, with some clusters incompletely filled with RyRs, and with a large fraction of clusters closely spaced within 20–50 nm, suggesting that smaller clusters may act together to function as a single site of CICR[10, 11].

During the initial depolarization stages of the action potential (AP), LCCs open allowing for the entry of Ca^{2+}. This inward flux of Ca^{2+} contributes to maintenance of the plateau phase of the AP. As Ca^{2+} concentration in the dyad increases, Ca^{2+} binds to the RyRs, increasing their open probability. Opening of RyRs leads to Ca^{2+} release from the JSR. The amount of Ca^{2+} released from the JSR is significantly more than the amount of trigger Ca^{2+} entering via LCCs[12]. The ratio of release to trigger flux of Ca^{2+} is known as ECC gain. The Ca^{2+} release flux is a smooth, continuous function of trigger influx, a behavior observed originally by Fabiato et al[13] and known as graded Ca^{2+} release. The resulting rapid, large increase in dyad Ca^{2+} concentration ($[Ca^{2+}]_d$) leads to Ca^{2+} diffusion from the dyad into the cytosol. As cytosolic Ca^{2+} concentration ($[Ca^{2+}]_c$) increases, Ca^{2+} binding to troponin C in the myofilaments initiates contraction of the myocyte.

Several mechanisms exist to remove trigger Ca^{2+} from the myocyte, and for re-uptake of released Ca^{2+} back into the NSR. During diastole, the Na^+-Ca^{2+} exchanger (NCX) is believed to import three Na^+ ions for every Ca^{2+} ion extruded, yielding a net inward charge movement[14] (see[15] for recently proposed alternative transport modes). It is the principal means by which Ca^{2+} is extruded from the myocyte. It can also function in reverse mode during the AP, in which case it extrudes Na^+ and imports Ca^{2+}.[16] The duration of reverse mode NCX, and hence its effect on AP shape, has been shown to vary with species, heart failure, and other factors[17, 18]. The sarcolemmal Ca^{2+}-ATPase also transports Ca^{2+} out of the cell, but flux through this pathway is small (2–3%) relative to other pathways[19]. The major mechanism by which released Ca^{2+} is transported back into the SR is the SR Ca^{2+}-ATPase (SERCA pump). Phospholamban (PLB) is normally bound to the SERCA pump, inhibiting its activity. Phosphorylation of PLB functionally up-regulates SERCA by increasing its Ca^{2+}-affinity[1, 20]. Density of the SERCA pump is highest in NSR. JSR refilling occurs via Ca^{2+} diffusion from the NSR. As each of these mechanisms restores $[Ca^{2+}]_c$ to diastolic values, Ca^{2+} dissociates from troponin C, terminating the contraction phase of the cardiac cycle.

The elucidation of CICR mechanisms has become possible with the development of experimental techniques for simultaneous measurement of L-type Ca^{2+} current (I_{CaL}) and Ca^{2+} transients, and detection of local Ca^{2+} release events known as Ca^{2+} sparks[21, 22]. As indicated by Soeller and Cannell[23], the tight regulation of SR Ca^{2+} release by triggering LCC current became evident with the following observations: (1) ECC gain is ~10 in response to a voltage clamp to 0 mV[24, 25]; (2) The magnitude of SR release is a smoothly graded function of I_{CaL} amplitude[25, 26]; and (3) the bell-shaped voltage-dependence of SR release is similar to that for I_{CaL}, but with its peak shifted in the hyperpolarizing direction by

~ 10 mV[25, 26]. These experimental observations gave rise to and later verified the local control theory of EC coupling. The mechanism of local control predicts that within discrete regions of the dyadic cleft, the opening of an individual LCC will trigger Ca^{2+} release from a small cluster of RyRs that reside in close proximity directly across the dyad. Tight regulation of CICR is achieved because LCCs and RyRs are regulated by $[Ca^{2+}]_d$ rather than by $[Ca^{2+}]_c$. The amplitude and profile of the whole-cell intracellular Ca^{2+} transient results from the recruitment and temporal summation of the elementary Ca^{2+} spark release events. The recruitment of Ca^{2+} sparks via this mechanism allows for graded control of SR Ca^{2+} release[27].

Many advances in integrative modeling of the ventricular myocyte have resulted from quantitative modeling of these components which underlie CICR and ECC in cardiac myocytes. In this review, we will present a range of models that have been developed to understand properties of CICR and ECC in the cardiac ventricular myocyte. We have chosen to focus on development of major new functional components of CICR and ECC, their integration into whole-cell models, and the insights that have been obtained from these advances in modeling capabilities that span multiple biological scales.

Common pool models of CICR

The landmark DiFrancesco-Noble model of the cardiac Purkinje fiber[28] was developed from the preceding Beeler-Reuter model[29] (first computational model of the cardiac ventricular myocyte) and that of McAllister et al[30]. This model was ground breaking for many reasons and was the first model to introduce descriptions of the transport of Ca^{2+} into the NSR by SERCA, extrusion of Ca^{2+} from the cytosol by NCX, diffusion of Ca^{2+} from NSR to JSR, and CICR from the JSR. This model established the conceptual framework on which all subsequent models of the myocyte have been built. While this model did reproduce graded SR Ca^{2+} release, it did so with ECC gain that was non-physiologically low.

The construction of mechanistic mathematical models of CICR which attempt to capture both high gain and graded SR Ca^{2+} release first lead to a series of “common pool” models, which, in fact, fail to capture these fundamental properties. As defined by Stern[27], common pool models are those in which LCC trigger Ca^{2+} enters the same Ca^{2+} pool into which JSR Ca^{2+} is released, and which controls JSR Ca^{2+} release. The rapid increase of Ca^{2+} in this pool leads to non-physiological regenerative, all-or-none rather than graded Ca^{2+} release, a situation where whole-cell SR Ca^{2+} release escapes control by I_{CaL} once it is initiated[26]. An additional assumption inherent in this type of model is that the gating dynamics of the entire population of RyRs are controlled by properties of whole-cell I_{CaL} rather than by properties of local LCC channel gating. Stern elegantly demonstrated via the application of linear stability theory that common pool models cannot achieve both high gain and graded Ca^{2+} release[27].

Regardless of this limitation of common pool models, many advances in cardiac myocyte modeling over the past decade have stemmed from improved descriptions of CICR in such models. The Jafri et al[31] model of the guinea pig ventricular myocyte was the first to incorporate a Markov model of the LCC (Fig. 1A) into an integrated myocyte model with mechanistic ECC. The LCC model was based on the concept of modal gating introduced by Imredy and Yue[32] based on single-LCC recordings in which Ca^{2+} induced a shift in LCC gating dynamics into a low open probability mode. The model contains subsets of states which reproduce channel behavior prior to (mode-normal), and following (mode-Ca) the occurrence of Ca^{2+} dependent inactivation (CDI). Openings are rare in mode-Ca, effectively inactivating the channel. Successive LCC models have incorporated the concept of modal gating in Markov models for describing LCC inactivation[33–35] as well as other modes such

as phosphorylation[36]. The Jafri et al[31] model was also first to implement a "restricted subspace", a single compartment representing the total volume of all dyads into which all Ca^{2+} flux through RyRs and LCCs is directed. This model made a number of predictions regarding mechanisms of CICR and Ca^{2+} cycling (reviewed in[37]). A major prediction of this model was that experimentally measured interval-force (transient) and frequency-force (steady-state) relationships could be explained by the interplay between RyR inactivation and SR Ca^{2+} load dynamics. This Ca^{2+}-subsystem was modified for canine in the model of Winslow et al[38] from which a model of heart failure was developed based on data obtained from myocytes isolated from dogs with tachycardia pacing-induced heart failure[39]. The model predicted that in heart failure, down-regulation of the SERCA pump and up-regulation of NCX decreased JSR Ca^{2+} load, Ca^{2+} release via the RyRs, and the strength of I_{CaL} CDI. The resulting increase in I_{CaL} acted to prolong AP duration (APD), a characteristic phenotype of heart failure. The model predictions were subsequently validated by experimental studies[40, 41], thereby demonstrating that negative feedback on LCCs by Ca^{2+} release from RyRs can exert significant control of AP properties. Furthermore, the heart failure model could produce early after depolarizations (EADs), a cellular arrhythmia believed to be a possible trigger for arrhythmia at the whole heart level. Upon introduction into a model of the ventricles, the EADs in the heart failure model quickly led to degeneration of electrical propagation into a cardiac arrhythmia, whereas the control myocyte model yielded normal coordinated ventricular activation during pacing.[42]

Despite the fact that these common pool models were not able to reproduce graded SR Ca^{2+} release, they were able to reproduce and predict many important behaviors of the cardiac ventricular myocyte, raising the question of whether capturing the mechanisms of graded release is of primary importance. One way to circumvent this issue is to model SR Ca^{2+} release flux as a phenomenological function of LCC influx and/or membrane potential. Doing so removes the positive feedback effect inherent to common pool models. Models incorporating a phenomenological mechanism of CICR have been successful in describing many myocyte behaviors (including the widely utilized models of Rudy and colleagues[43, 44]). However, as with any phenomenological model, care must be taken when interpreting results of these models that pertain to Ca^{2+} release. The critical relationship between SR Ca^{2+} release and APD[38, 40, 41], and the recognition that the feedback of SR Ca^{2+} release on LCCs occurs locally in discrete Ca^{2+} spark events[21] suggested that capturing the mechanisms of local interaction between LCCs and RyRs would be essential. Furthermore, experimental data were emerging that supported the idea that LCC inactivation was dominated by CDI rather than voltage-dependent inactivation (VDI)[45–47]. Strong CDI in combination with weak/incomplete VDI causes instability in common pool models[34] (which were therefore typically formulated with strong VDI and weak CDI) because all-or-none SR Ca^{2+} release induces fast whole-cell CDI which eliminates the late phase of I_{CaL} and destabilizes the AP plateau (see Fig. 10C of ref[34]). This made it clear that in order to fully capture the core mechanisms of ECC, a model in which LCCs locally control RyR function was needed.

Local control of SR Ca^{2+} release

In 1992, Stern[27] formulated idealized models of "local control" of CICR, and in doing so advanced the local control theory of ECC which underlies how the microscopic properties of CICR translate into macroscopic physiologic phenomena observed in experiments. The approach was to recognize that the non-physiologic positive feedback loop inherent in common pool models of CICR must be broken by separating Ca^{2+} released from the SR from the trigger Ca^{2+} influx. This was accomplished by noting that LCCs and RyRs reside in close apposition on opposite sides of the dyadic cleft, which would effectively grant Ca^{2+} ions permeating an LCC privileged access to the Ca^{2+} binding sites on nearby RyRs.

Importantly, the assumed structural separation of individual clefts[8] means that released Ca^{2+} would not generally act as a trigger to RyRs in distant dyads (though recent studies suggest neighboring RyR clusters may have a functional role in ECC[11, 48]). Stern's "calcium-synapse" model, in which each dyad was assumed to contain a single LCC and a single SR release channel, captured these ideas in an elegantly simple way, demonstrating that high gain and graded SR release arise from the local correlation in stochastic LCC and RyR gating due to their communication via a common local Ca^{2+} signal. In this model, graded release is achieved by statistical recruitment of elementary SR Ca^{2+} release events. This fundamental idea of local control of SR release spurred a number of modeling studies, some of which focused on detailed dynamics of Ca^{2+} distribution within the dyadic junction, some of which focused on mechanisms of Ca^{2+} release termination, and a small handful of which developed fully integrative models that relate macroscopic cellular properties of ECC to the function of independent, locally controlled Ca^{2+} release units.

Due to the small size of the dyad, it became clear that understanding the spatial and temporal profile of $[Ca^{2+}]_d$ would be an important step in elucidating the mechanistic details of local CICR. Langer and Peskoff[49] developed one of the first detailed models to numerically simulate the time course of dyadic Ca^{2+}. The model predicted that a single typical LCC opening led to ~ 1 mmol/L $[Ca^{2+}]_d$ near the mouth of the LCC. The presence of sarcolemmal buffering sites slowed the decay of the local Ca^{2+} transient (such that it remained highly elevated long after LCC closure) as compared to the dynamics in the absence of buffers, a finding which was inconsistent with the idea that LCC gating imposes tight control on RyR activity. Soeller and Cannell[50] formulated a dyad model which introduced the electrostatic effects of ion movement which predicted that $[Ca^{2+}]_d$ actually changes more rapidly in response to LCC gating. In this model, $[Ca^{2+}]_d$ was approximately proportional to unitary LCC currents over a wide range of current amplitudes. The model yielded predictions of $[Ca^{2+}]_d$ profiles during JSR release, which peaked as high as 300 μmol/L near the center of the dyad. The decay in dyadic Ca^{2+} occurred in ~ 2 ms following termination of SR release (but this was sensitive to the dyad boundary condition). The high speed of the response of dyadic Ca^{2+} to LCC and RyR gating in this model helped to explain how tight local control of SR release by LCCs can be achieved.

With the growing acceptance of local control theory of CICR and that Ca^{2+} sparks are the elementary events underlying SR Ca^{2+} release (for a review see[51]), mathematical models of Ca^{2+} sparks were developed. The summation of Ca^{2+} sparks could explain the characteristic properties of CICR, ECC gain, and whole-cell Ca^{2+} transients, therefore the analysis of models of single Ca^{2+} sparks and ensembles of Ca^{2+} sparks provided a wealth of information. Local control of CICR requires that SR release be stable, which suggests that Ca^{2+} sparks, which are locally regenerative, must be terminated rapidly by a robust mechanism. While the mechanisms of Ca^{2+} spark termination still remain unclear, a number of models have helped elucidate how possible mechanisms may contribute to termination of SR Ca^{2+} release.

Stern[27] originally described three mechanisms that can terminate SR release in a cluster of RyRs: (1) RyR inactivation is a time-dependent process which may be initiated by Ca^{2+} binding to an inactivation site on the RyR or may occur "fatefully" following opening of the channel. The observed inactivation process has been described as classically inactivating (leading to absolute refractoriness of CICR)[52] or taking on the complex properties of adaptation[51]. (2) Depletion of locally releasable JSR Ca^{2+} will occur as the result of RyR activity. The emptying of the cisternal Ca^{2+} store reduces the Ca^{2+} gradient across the RyRs, and hence the Ca^{2+} flux. This will diminish the local feedback that underlies regenerative release in a cluster of RyRs, allowing them to close. (3) "Stochastic attrition" occurs as a result of the non-zero probability that all RyRs in a cluster are simultaneously closed. Since

Ca^{2+} diffuses rapidly out of the dyad, the simultaneous closure of all RyRs would lead to a rapid reduction in $[Ca^{2+}]_d$ below the level which sustains RyR activity. Active RyR clusters would therefore gradually cease gating spontaneously. This mechanism can only be effective on a reasonable timescale if very few RyRs are activated during a Ca^{2+} spark, and it does not provide for a mechanism of refractoriness. The stereotypic nature of Ca^{2+} spark properties suggested that spark generation and termination are likely controlled by regulatory feedback mechanisms and cannot be described by a simple stochastic mechanism alone[23]. An additional mechanism proposed recently is RyR regulation by luminal SR Ca^{2+}. RyR sensitivity to $[Ca^{2+}]_d$ can be altered by the level of JSR luminal $[Ca^{2+}]$ via the interaction of the Ca^{2+} buffer calsequestrin with RyR accessory proteins triadin and junction within the JSR[53]. The decrease in RyR open probability with JSR depletion likely contributes to termination of Ca^{2+} release.

In 1999, Stern et al[33] developed a stochastic model of cardiac ECC. The model consisted of a cardiac dyad in which the Ca^{2+} concentration profile was simulated by solving equations governing diffusion and Ca^{2+} binding reactions in the cleft. LCCs and RyRs were represented by Markov state models, which were simulated as part of a stochastic system in which the state of each individual channel was tracked. The behavior of six different RyR gating schemes was analyzed in the context of local control of ECC. This study revealed that local control, in a realistic setting of dyad geometry, number, and location of channels, could explain graded release, when the RyR was represented by a simple phenomenological four-state gating scheme which included inactivation (Ca^{2+}-dependent or fateful). This success has led to continued development of this RyR model in more recent work[54, 55]. However, RyR channel gating schemes that were based on single-channel RyR measurements in lipid bilayers[56, 57] failed to give stable ECC (but stability could be restored by introducing allosteric RyR interactions[33]). The work of Stern et al[33] suggested that there must be a sufficiently strong process that substantially reduces RyR open probability shortly following activation such that stochastic attrition can occur on the timescale of physiological ECC.

Whether or not RyR inactivation or adaptation plays an important role in termination of SR Ca^{2+} release remains controversial (see below). A number of RyR models[57, 58] were developed to better understand the observation of RyR adaptation[59], whereby an RyR can reopen in response successive increases in Ca^{2+} concentration, indicating they have not entered a conventional absorbing CDI state. Rice et al[60] developed a stochastic model of Ca^{2+} release in the dyadic junction which demonstrated that RyR adaptation modulated Ca^{2+} release duration and amplitude but was not required for termination of Ca^{2+} release (i.e. JSR depletion played an important role). This model achieved high gain and graded release without tracking the spatial gradients of $[Ca^{2+}]_d$. In contrast, the RyR model of Shannon et al[54] is a modification of the phenomenological four-state model of Stern et al[33], which introduced an important modulatory role for SR luminal Ca^{2+} in RyR gating but which still depends upon an inactivation/adaptation mechanism for release termination. Variations of this model have been incorporated into a variety of recent models which have successfully described SR load and frequency dependent properties of ECC and APs in rabbit[54] and human[61], the role of RyR phosphorylation on Ca^{2+} dynamics and the AP[55], and the role of spatial coupling between dyadic release sites in Ca^{2+} spark-induced sparks and Ca^{2+} alternans[48].

In 2002, Sobie et al[62] developed a Ca^{2+} spark model to further investigate mechanisms underlying termination of SR Ca^{2+} release. In this model each release site is composed of a large number of two-state RyRs which incorporate two additional experimental observations: (1) elevated SR luminal Ca^{2+} increases the Ca^{2+}-sensitivity of RyR activation[63], and (2) RyR coupling cooperatively influences their gating properties within a cluster[64]. These mechanisms of RyR gating yield a “sticky cluster” model which reproduces

fundamental features of Ca^{2+} sparks and robust termination of release that arises as a result of the combined effects of these two mechanisms. In this model, the assumption of coupled RyR gating is essential for reliable SR release termination. However, it remains unclear how RyRs would influence the gating properties of all other RyRs in a cluster (as opposed to only adjacent RyRs[33]) as implemented in this model (see [65, 66] for alternative approaches to modeling the functional effects of RyR coupling). In addition, the >90% SR depletion required for release termination in the Sobie et al[62] model may not be realistic as experiments have demonstrated that 40–75% of releasable Ca^{2+} remains in the JSR following whole-cell triggered SR release[67, 68]. Despite these issues, the majority of recent experiments[68–70] have strengthened the idea that termination of SR release is primarily controlled by luminal SR Ca^{2+} rather than an RyR inactivation mechanism.

While many controversies as to the details of CICR remain to be resolved, the models of dyadic Ca^{2+} dynamics, Ca^{2+} sparks and CICR have helped affirm or disprove a variety of mechanistic hypotheses regarding cardiac ECC. Most of these ECC models, however, have been implemented at the sub-cellular scale, isolated from the physiological environment and influence of other cellular processes. The first mathematical model to incorporate the mechanisms of local control of SR Ca^{2+} release at the level of the cardiac dyad into an integrative model of the cardiac action potential was published in 2002 by Greenstein and Winslow[34] (Greenstein-Winslow model). This model is described in detail below in the section “Multi-scale modeling of CICR”.

Multi-scale modeling of CICR

Quantitative understanding of CICR requires that Ca^{2+} signaling be understood across a wide range of spatio-temporal scales. The length-scale over which CICR occurs within the dyad is on the order of nanometers, and relevant time-scales are of the order of microseconds. Integration to the level of the cell requires formulation of models that describe behavior at spatio-temporal scales of several hundred microns and tens to hundreds of seconds. Recently, we have developed several new approaches for multi-scale modeling of CICR spanning these spatio-temporal scales[34, 71–73]. In this section, we present these models and the mathematical techniques for moving across these spatio-temporal scales.

The Nano-Scale Model of CICR

We have recently developed a computational model of Ca^{2+} signaling in the dyad that simulates motion of Ca^{2+} ions, binding of ions to RyR receptor sites, and Ca^{2+} release from RyR. This model was developed in order to understand factors shaping CICR at the nano-scale level. We addressed the following three questions: 1) what is the number of Ca^{2+} ions that are present in the dyad during CICR?; 2) how does the physical arrangement of large proteins within the dyad influence CICR?; and 3) how does “signaling noise” due to the potentially small number of Ca^{2+} ions within the dyad affect the nature of CICR? We addressed these questions by developing a molecularly- and structurally-detailed computational model of the cardiac dyad describing motions of Ca^{2+} ions, as influenced by thermal energy and electrostatic potentials.

The small size of the dyadic cleft (~ 4×10^5 nm^3 with ~ 10–40 RyRs)[10, 11], in combination with the relatively large proteins that reside in the cleft, results in a space in which Ca^{2+} diffusion is highly restricted. Figure 1B shows a representation of an LCC, RyR, and a single calmodulin (CaM) molecule in the dyad based directly on structural data[74–76]. Models predict that during an AP, peak Ca^{2+} concentration in the dyad ranges from 100 to 1,000 μmol/L[49, 50], which corresponds to as few as 20–200 free Ca^{2+} ions[73]. Therefore, application of laws of mass-action to analysis of signaling events mediated by this relatively small number of ion may not be justified[77]. Rather, the stochastic motion of Ca^{2+} ions in the

dyad may impart a degree of signaling noise between LCCs and RyRs, thereby influencing properties of CICR[73]. In addition, the physical location and dimensions of dyad proteins may have considerable influence on motion of Ca^{2+} ions and hence, CICR.

Development of the nano-scale model is presented in detail elsewhere[73]. Briefly, a simplified dyad was modeled using a 200 nm × 200 nm × 15 nm lattice containing 20 RyRs arranged in a 4 × 5 matrix. Four LCCs were positioned randomly across this lattice to achieve a 5:1 RyR:LCC ratio. The geometry of each LCC and RyR protein was modeled as shown in Fig. 1B, with each LCC tethering with one CaM. LCC gating was simulated stochastically using the model of Fig. 1A. The gating kinetics of the RyR were described using the four-state Markov model of Stern[33,78]. Entry of Ca^{2+} ions into the dyad via open LCCs and RyRs was modeled as a Poisson process with rate governed by channel permeabilities measured experimentally[79]. CDI of an LCC required that the two carboxyl-terminal Ca^{2+} binding sites of the associated CaM were occupied. Opening of an RyR required that Ca^{2+} was bound to all four activation sites. RyRs were assumed to inactivate when Ca^{2+} was bound to at least one out of four distinct inactivation sites. Sarcolemmal anionic sites acted as Ca^{2+} buffers[49, 50]. The joint positions of Ca^{2+} ions present in the dyad were modeled as a Brownian motion in a potential field, describing both interactions of Ca^{2+} ions with other Ca^{2+} ions as well as electrostatic potentials based on the Fokker-Planck equation (FPE)[80]. We generated sample paths of Ca^{2+} ion movement in the dyad using a finite difference representation of the FPE that can be interpreted as a spatially discrete Markov process as described by Wang et al[81].

A 10 ms simulation of a model dyad containing only one LCC located at its center at a membrane potential of 0 mV generated an average of ~ 0.5 Ca^{2+} ions within a 50 nm radius of the LCC (see Fig. 8 of[73]), with a minimum of zero and a maximum of 7 Ca^{2+} ions, corresponding to 98.7 μmol/L $[Ca^{2+}]_d$. A similar protocol using a single RyR in the SR membrane (in which the RyR is initially open) generated an average of ~ 22.8 Ca^{2+} ions. The number of Ca^{2+} ions peaked at 49 during Ca^{2+} release, which corresponds to a concentration of ~ 0.7 mmol/L Ca^{2+}, similar to the concentration of Ca^{2+} found in the JSR[82]. With a coefficient of variation of 64%, RyR gating produces a high degree of variability in the number of dyadic Ca^{2+} ions, showing that the LCC-RyR signaling involved in CICR at the dyad level is a noisy process mediated by tens of Ca^{2+} ions.

Panels A and B of Figure 2 demonstrate fundamental features of a representative Ca^{2+} release event in a dyad in response to a voltage clamp to 0 mV at time zero. Panel A shows the number of Ca^{2+} ions in the dyad, and panel B shows the number of LCCs (gray line) and RyRs (black line) that are open as a function of time during the release event. Two LCCs open at ~ 3 ms following the voltage clamp, and Ca^{2+} influx into the dyad triggers the opening of 3 RyRs 1–2 ms later, which inactivate after ~ 7 ms, ~ 9 ms, and ~ 13 ms, respectively. The temporal shape of the Ca^{2+} signal in the dyad (Fig. 2A) is closely correlated to the number of open RyRs (Fig. 2B). Figure 2C shows the average dyadic Ca^{2+} signal, calculated by averaging the number of Ca^{2+} ions at each point in time across 400 independent dyads. The duration of the average local Ca^{2+} transient shown in Panel C is ~ 20 ms (at half-maximal amplitude), similar to that measured for Ca^{2+} spikes in myocytes[21, 24, 52].

We demonstrated that ECC gain is a robust and reproducible measurement of CICR because the variability in gain that arises from the stochastic gating of LCCs and RyRs is small for a whole-cell population of dyads at potentials near and above 0 mV (see Fig. 11 of[73]). The functional influence of protein structures on ECC is shown in Fig. 2D. Peak ECC gain obtained for the baseline model (solid line) is compared to that for the model in which LCC, RyR, and CaM molecule structures were omitted (dashed line). Ca^{2+} binding site locations

for the no-structure simulations remain at the same positions in space as when the protein structures are in place. Over a wide range of potentials, the peak ECC gain is decreased upon removal of the protein structures from the dyad. The protein structures occupy ~ 15% of the dyad volume. In order to show that the difference in ECC gain in the presence vs. absence of protein structures is not simply attributable to the difference in Ca^{2+}-accessible dyad volume, peak ECC gain was obtained with protein structures absent and dyad volume reduced by ~ 15% (dotted line). ECC gain values for this model were clearly are not increased to the level obtained in the presence of protein structures. These data indicate that the physical shape and configuration of dyad proteins influences Ca^{2+} diffusion during CICR in such a way as to enhance ECC gain. In addition, the probability of triggering a release event was 0.152 with protein structures excluded and 0.105 with protein structures intact, a 44% increase. These data suggest that when LCCs are directly apposed to RyRs, the diffusion obstacle imposed by the structure of RyRs leads to an increase in the probability that trigger Ca^{2+} ions bind to activation sites on the RyRs, and hence increases ECC gain.

These data demonstrate that at the level of single dyads, CICR is a highly noisy process and that models based on laws of mass action may not accurately capture dyadic Ca^{2+} dynamics. Further, in ensembles of dyads, the fundamental properties of local control of CICR arise *de novo* as a consequence of the underlying physical structure and channel gating properties, including voltage-dependence of ECC gain. Finally, the physical shape and location of RyRs relative to LCCs is likely to have a major influence on properties of CICR.

The Integrated Local-Control Model of the Cardiac Myocyte

The Greenstein-Winslow[34] model of the cardiac ventricular myocyte was the first to fully integrate mechanisms of local control of CICR into a model of the cardiac AP. This was accomplished by updating and extending the common-pool model of Winslow et al.[38] to include a population of dyadic Ca^{2+} release units (CaRUs). In essence, this integrated local control model is generated from the nano-scale model by simplifying the dyad description to that of well-mixed Ca^{2+} compartment, and incorporating a large population of such dyads into a whole-cell model. Detailed properties of the nano-scale model (e.g. effect of protein structure on ECC gain) are retained in this integrated model by adjusting parameters that influence the effectively equivalent property at this scale (e.g. effective Ca^{2+} sensitivity of RyRs). In this model, local interactions of individual LCCs with nearby RyRs are simulated stochastically, with these local simulations embedded within the numerical integration of the ordinary differential equations (ODEs) describing ionic and membrane pump/exchanger currents, SR Ca^{2+} cycling, and time-varying cytosolic ion concentrations.

The Greenstein-Winslow model was formulated to capture fundamental properties such as graded release, while at the same time needed to be computationally tractable. A full mathematical description of the stochastic state models, dynamical equations, parameters, and initial conditions defining the myocyte model are given in Appendix I of [34]. Figure 3A shows a schematic of the CaRU model which is intended to mimic the properties of Ca^{2+} sparks in the t-tubule/SR (T-SR) junction. Figure 3B shows a cross-section of the model T-SR cleft, which is divided into four individual dyadic subspace compartments arranged on a 2 × 2 grid. Each subspace compartment contains a single LCC and 5 RyRs in its JSR and sarcolemmal membranes, respectively[83]. The division of the CaRU into four subunits allows for the possibility that an LCC may trigger Ca^{2+} release in adjacent subspaces (i.e., RyR recruitment). Upon activation of RyRs, subspace $[Ca^{2+}]$ will become elevated. This Ca^{2+} freely diffuses to either adjacent subspace compartments (J_{iss}) or into the cytosol (J_{xfer}). The local JSR compartment is refilled via passive diffusion of Ca^{2+} from the NSR compartment (J_{tr}). The number of active LCCs was chosen such that the amplitude of the ensemble current summed over all LCCs corresponds to whole-cell measurements in canine myocytes[84] which corresponded to 50,000 LCCs (12,500 CaRUs) and agrees with

experimental estimates of LCC density[79]. LCC and RyR gating were based on previous models[31, 85], and the channels (ClCh) that carry the Ca^{2+}-dependent transient outward chloride (Cl^{-}) current (I_{to2}) are included within the CaRU.[86] A detailed description of the local control simulation algorithm is given in Appendix II of [34]. Stochastic fluctuations in model outputs are the natural result of the ensemble behavior of ion channel and CaRUs, and introduce a degree of variability to simulation output and can be physiologically important to understanding some physiological phenomena such as EADs[87].

Panels A and B of Fig. 4 demonstrate the most elementary model release event during CICR, as triggered by a single LCC at 0 mV. Ca^{2+} flux through an LCC (gray line) and the net SR Ca^{2+} release flux through the five adjacent RyRs (black line) are shown in Fig. 4A. Local JSR release flux is triggered by the first LCC opening (at ~ 5 ms) and lasts ~20 ms, far longer than the LCC open duration (<1 ms). The amplitude of the release flux varies with the number of open RyRs and the local Ca^{2+} gradient across the JSR membrane. Figure 4B shows the corresponding subspace [Ca^{2+}], which reaches a peak value of ~ 40 μmol/L. Total Ca^{2+} influx through the set of four LCCs (gray line) and the net SR Ca^{2+} release flux through the set of 20 RyRs (black line) that make up a single T-SR junction are shown in Fig. 4C. LCC Ca^{2+} influx rises to a level consistent with two open channels within a short time following the initiation of the pulse. The spatial average of Ca^{2+} concentration in the four subspace compartments of the CaRU is intended to represent a Ca^{2+} spark-like event (Fig. 4D), and has duration of 25 ms (at half-maximal amplitude) similar to that measured in myocytes (20–50 ms) [21, 24, 52].

Previous experimental studies[25, 88] and mathematical models[27, 33] have shown significant differences between the voltage dependence of I_{CaL} and RyR Ca^{2+} release flux even though SR Ca^{2+} release is exclusively controlled by LCC Ca^{2+} entry. These differences underlie the phenomenon of “variable” EC coupling gain. Figure 5A shows the voltage dependence of LCC (filled circles) and RyR (open circles) Ca^{2+} flux. In Fig. 5B, the peak fluxes of Fig. 5A have been normalized based on their respective maxima. Maximal LCC Ca^{2+} influx occurs at 10 mV, whereas maximal RyR Ca^{2+} release flux occurs at 0 mV. EC coupling gain is plotted as a function of voltage in Fig. 5C (triangles), and is monotonically decreasing with increasing membrane potential in agreement with experimental measurements[24, 25, 88]. In the negative voltage range LCC open probability is submaximal, leading to sparse LCC openings (i.e. submaximal recruitment of CaRUs), but large amplitude unitary currents efficiently trigger adjacent RyRs, resulting in high values of ECC gain. More CaRUs are recruited with increasing membrane potential as a result of increasing LCC open probability, however ECC gain decreases with increasing membrane potential because the higher LCC open probability leads to redundancy in LCC openings as a result of which a fraction of LCCs are attempting to trigger refractory RyRs and at even higher potentials the decrease in LCC unitary current amplitude reduces the fidelity of local coupling between LCCs and RyRs.

Figure 6 demonstrates the ability of the Greenstein-Winslow model to reconstruct APs and cytosolic Ca^{2+} transients of normal canine midmyocardial ventricular myocytes. In Fig. 6A, a normal 1-Hz steady-state AP is shown (solid black line). AP properties are similar to those measured in experiments[39], with APD of ~300 ms. Also shown in Fig. 6A are the kinetics of CDI (dashed line) and VDI (dotted line), demonstrating that this model conforms with experimental findings that indicate LCC CDI is strong while VDI is relatively slow and incomplete[46, 47]. Figure 6B shows cytosolic (black line) and mean subspace (gray line) Ca^{2+} transients. The cytosolic Ca^{2+} transient peaks at ~ 0.75 μmol/L and lasts longer than the duration of the AP whereas Ca^{2+} in the subspace reaches ~11 μmol/L on average, and equilibrates to near-cytosolic levels rapidly, within ~ 100 – 150 ms. The simulations of Figs.

4–6 demonstrate that this multi-scale model faithfully reproduces a variety of experimental observations that span from single-channel to whole myocyte.

The Coupled LCC-RyR Local Control Model

A limitation of the Greenstein-Winslow[34] local control model is that it is far more computationally demanding than deterministic models. To address this, we recently developed an analytical "first-principles" approach for deriving simplified mechanistic models of CICR by applying a carefully chosen set of approximations that allow for the ensemble behavior of CaRUs to be represented by a low dimensional system of ODEs, eliminating the need for computationally expensive stochastic simulations. This model, termed the coupled LCC-RyR model[72], retains the biophysically based description of local control of CICR, and captures its key properties including graded SR Ca^{2+} release and voltage dependent ECC gain and is the basis of a deterministic local control model of the cardiac myocyte[71].

Following the methods described by Hinch et al[72], LCC and RyR models composed of the minimum number of states necessary to capture fundamental dynamics of channel gating were designed and constrained based on experimental data sets. A simplified CaRU model consisting of only a single LCC and a single RyR was formed. The relatively fast diffusion (i.e. short diffusion distance) of Ca^{2+} from dyad to cytosol (as compared to the time scale of LCC and RyR gating)[62] allows for the application of a steady state approximation for dyadic Ca^{2+} diffusion. This allows the resulting CaRU to be analytically simplified into a single Markov state model in which each state represents a unique configuration of channel states for the combined set of LCCs and RyRs in the CaRU. In the resulting formulation, the dynamics of a population of CaRUs can be described by a deterministic set of coupled ODEs. Other elegant methods have been derived to improve computational efficiency of ECC simulations as well[37, 89, 90], but have not yet been implemented in an integrated myocyte model using biophysically detailed channel models.

Panels D–F of Figure 5 demonstrate that the deterministic coupled LCC-RyR model reproduces the fundamental quantitative properties of CICR in a similar manner to its stochastic predecessor[34] in panels A–C. The effect of dyad size on ECC was analyzed using models with 2-fold and 3-fold larger dyads (Fig. 5F, gray and dashed lines, respectively). In each case the number of dyads per cell was reduced such that the total number of LCCs and RyRs per cell was conserved, and the RyR/LCC stoichiometry was unchanged. At potentials more negative than −10 mV, the increase in CaRU size yields a substantial increase in gain such that the ECC gain curve acquires the steep slope similar to those observed experimentally[24, 25]. This arises as a result of a model-dependent increase in the functional RyR/LCC ratio because it is likely that a single LCC opening will trigger regenerative release from most RyRs in a CaRU. The coupled LCC-RyR local control model reconstructs APs and Ca^{2+} transients of canine midmyocardial ventricular cells (see Fig. 6 of [71] for details) at a variety of pacing frequencies, and similar to the Greenstein-Winslow model, has an I_{CaL} which exhibits strong CDI and weak VDI. The ability of this model to reproduce all of the core features of the stochastic local control model in an efficient manner has made it a candidate for use in large scale tissue simulations[91].

Additional domains of localized Ca^{2+} signaling

There have been a number of recent models in which Ca^{2+} signaling in localized compartments other than the dyad have been investigated. Experimental measurements of NCX current[18] have provided evidence that this transport mechanism, and possibly the sarcolemmal Ca^{2+}-ATPase, may be driven by subsarcolemmal Ca^{2+}, which is elevated relative to Ca^{2+} concentration in the bulk cytosol as a result of Ca^{2+} diffusion limitations.

The rabbit ventricular myocyte model of Shannon et al[54] was the first to introduce a subsarcolemmal Ca^{2+} compartment, and a number of recent models now include a subsarcolemmal Ca^{2+} compartment[35, 61, 92, 93]. Elevated subsarcolemmal Ca^{2+} may have a particularly important influence on NCX. It has been suggested that elevated subsarcolemmal Ca^{2+} during the early phase of the AP may modulate NCX reversal potential, reducing entry of Ca^{2+}.[94] More needs to be done to quantify the functional consequences of sensing subsarcolemmal Ca^{2+} and NCX function. This is particularly important given the role of NCX in shaping AP properties and its possible role in the generation of delayed after-depolarizations. Very interestingly, the Pasek et al[95] model of the guinea pig ventricular myocyte includes a diffusive t-tubule system with a heterogeneous distribution of ion channels between tubular and surface membranes, thus introducing a new *extracellular* compartment. This model predicted that Ca^{2+} depletion and K^+ accumulation in the t-tubule during APs leads to a reduction in SR Ca^{2+} load, which would impact ECC.

There is now substantial electrophysiological evidence that extra-dyadic processes also influence CICR. Evidence suggests that Ca^{2+} entry via reverse-mode NCX activity may either trigger or modulate CICR[96, 97] and that CICR modulates NCX function[98]. NCX has also been identified in the t-tubules at a high level. However, the precise location of NCX within[99] and/or near[100] the dyad remains uncertain. Lines et al[101] used a model of the cardiac dyad which accounted for details of both Ca^{2+} and Na^+ diffusion to demonstrate that if fast Na^+ channels are in the dyadic cleft then NCX (driven by the local elevation in $[Na^+]$) can influence the timing of local CICR. Recent evidence also suggests NCX may form a functional complex with NKA and its accessory protein phospholemman[102]. Furthermore, one study suggests that NCX and NKA constitute a physically interacting molecular complex with ankyrin-B and an inositol 1,4,5-phosphate operated Ca^{2+}-releasing channel ($InsP_3R$) in the t-tubules that is distinct from the LCC-RyR complex[100]. This hypothetical "ankyrin-B complex" may play an important role in the regulation of local Na^+ and Ca^{2+} concentrations and possibly modulate CICR by regulating the boundary conditions on dyadic Ca^{2+}. Again, it is likely that these regulatory interactions are mediated by small numbers of Ca^{2+} ions. This may be a common theme in cases where proteins interact over nanometer length scales.

Recent work also demonstrates that mitochondria are positioned near dyads[103, 104]. Electron-dense structures that link the mitochondrial outer membrane with JSR, NSR, and t-tubules have been observed. These structures appear to be preferentially located, with one population forming attachments to NSR, and another set of bridges being near the dyadic cleft. Attachments to t-tubules were observed, but were rare. Ca^{2+} is taken up by mitochondria via the mitochondrial Ca^{2+}-uniporter[105]. Therefore, spatial co-localization of mitochondria near the dyadic cleft may give rise to an additional Ca^{2+}-signaling micro-domain involved in the regulation of mitochondrial ATP production, and which modulates dyadic Ca^{2+} concentrations and Ca^{2+} diffusion between adjacent RyR couplons[106].

Regulation of CICR by cell signaling pathways

Cardiac proteins involved in CICR and ECC are primary targets for regulation via cell signaling pathways and models have played a key role in understanding this regulation (see accompanying article in this series by Yang and Saucerman). The Greenstein-Winslow[34] model was extended to study effects of the β-adrenergic signaling pathway by the incorporation of protein kinase A (PKA)-mediated functional changes in target proteins[107] and could explain PKA-mediated changes in AP shape, dissected the specific effects of PKA-mediated phosphorylation of LCCs and RyRs on the voltage-dependent gain of CICR, and predicted a mechanism by which increasing levels of LCC phosphorylation could lead to increased frequency of EADs[87]. Saucerman et al[108] developed a differential-algebraic

model of the β-adrenergic signaling pathway and incorporated it into the rabbit myocyte model of Puglisi et al[109] and used this model to quantitatively understand and predict effects of specific molecular perturbations on cAMP dynamics and contractility via changes in function of target proteins resulting from altered phosphorylation dynamics. Recently, the model of Saucerman et al[108] was incorporated into the guinea pig ventricular model of Faber and Rudy[110] in a study of the role of β-adrenergic agonists and antagonists in long-QT syndrome[111].

An important Ca^{2+} cycling regulatory mechanism of recent interest is the signaling pathway involving Ca^{2+}/CaM-dependent protein kinase II (CaMKII), whose targets proteins include LCCs, RyRs, PLB, and the SERCA pump, as well as Na^+ and K^+ channels[112]. Evidence suggests that CaMKII is directly associated with its target proteins[113, 114] (implying that CaMKII signaling occurs locally in the dyadic junction), and that CaMKII activity is elevated in heart failure[115]. The first model of the cardiac myocyte to integrate the role of CaMKII was presented by Hund and Rudy[43], which predicted that CaMKII plays an important role in the rate dependent properties of the cytosolic Ca^{2+} transient, but not APD. Saucerman and Bers[93] incorporated models of CaM, CaMKII, and calcineurin (CaN) into the Shannon et al[54] model in order to better understand the functional consequences of the different affinities of CaM for CaMKII and CaN during APs. The model predicted that in the cardiac dyad, Ca^{2+} levels lead to a high degree of CaM activity which results in frequency-dependent CaMKII activation and constitutive CaN activation, whereas the lower Ca^{2+} levels in the cytosol only minimally activate CaM, which allows for gradual CaN activation, but no significant activation of CaMKII. Grandi et al[116] developed a model of CaMKII overexpression in the rabbit ventricular myocyte, including the role of CaMKII phosphorylation of fast Na^+ channels, LCCs, and the transient outward K^+ current (I_{to1}), which revealed a net effect of APD reduction with CaMKII. Recently, Hashambhoy et al[36] described dynamic CaMKII phosphorylation of LCCs in an extension of the Greenstein-Winslow[34] model. In this model it is assumed that a single CaMKII holoenzyme is tethered to each LCC, each CaMKII monomer can transition among a variety of activity states (see Fig. 2 of Hashambhoy et al[36]), and CaMKII monomers can catalyze phosphorylation of individual LCCs. This model demonstrated that CaMKII-dependent shifts of LCC gating patterns into high activity gating modes may be the underlying mechanism of a variety of experimentally observed phenomena associated with I_{CaL} facilitation. Hashambhoy et al[55] further expanded this model to include CaMKII-dependent regulation of RyRs and demonstrated that under physiological conditions, CaMKII phosphorylation of LCCs ultimately has a greater effect on RyR leak flux and APD as compared with phosphorylation of RyRs (Fig. 7A). APD was shown to correlate well with a CaMKII-mediated shift in modal gating of LCCs (Fig. 7B).

Future Directions in ECC Modeling

A number of mechanistic questions remain unanswered in cardiac ECC. As noted above, controversy remains as to mechanisms involved in termination of SR Ca^{2+} release. The high degree of technical difficulty involved in experimentally assessing RyR and CaRU properties under physiological conditions has resulted in limited and difficult-to-reproduce measures of certain key features of CICR such as RyR gating properties (e.g. coupled gating of RyRs), the degree of local JSR Ca^{2+} depletion associated with Ca^{2+} sparks (Ca^{2+} blinks), and the rate of local refilling of JSR. Models have been able to reveal and demonstrate multiple possible mechanisms of SR Ca^{2+} release termination, but the lack of consensus on a single experimentally verified mechanism has allowed a variety of mathematical model formulations of SR Ca^{2+} release to coexist. Improved resolution of both structural and functional imaging of ECC domain ultrastructure and localized Ca^{2+} dynamics will help to resolve these questions and to further validate and refine nano- and microscale models of

ECC[10, 11]. Additional areas of recent interest, where mechanistic models have yet to be fully developed, include regulation of ECC by mitochondrial Ca^{2+} dynamics (see above) and functional alteration of key ECC proteins arising from oxidative-stress (e.g. effects of mitochondria-derived reactive oxygen species) associated with heart failure. Recently, Tadross et al[117] used a combination of elegant models and experiments to elucidate a mechanism underlying Ca^{2+} channel CDI, by which CaM in complex with an LCC, can sense and decode local and global Ca^{2+} signals. The implications of this mechanism on our understanding of dyadic Ca^{2+} dynamics and cardiac ECC have yet to be studied with models. Finally, the mathematical techniques used in developing models that span multiple biological scales are not adequate for all applications and themselves are an ongoing area of theoretical study (see ref [37] for a recent review of model reduction methods). Mechanistic model reproduction of phenomena such as Ca^{2+} alternans and delayed after depolarizations depend on the ability of a Ca^{2+} spark to trigger neighboring release sites and form intracellular Ca^{2+} waves[48]. While model reduction techniques have captured important features of local control of ECC (as described above), the lack of low-dimensional models that can capture Ca^{2+} wave mechanisms has made it difficult to extend such models to the tissue and whole heart level in order to study how these events trigger large scale arrhythmias. The development of models that can accomplish this task in a tractable formulation will greatly improve our ability to understand the mechanistic links between disease-related changes in ECC and arrhythmia.

Conclusion

Integrative modeling of cardiac ECC and myocyte physiology has played a critical role in revealing mechanistic insights at and across a range of biological scales. At the smallest scale, models have shed light on how Ca^{2+} ions and proteins in the cardiac junction interact during LCC and RyR gating. Expanding our view, simplified models of individual release sites have allowed for detailed simulations that reveal determinants of Ca^{2+} spark activation and termination properties. On an intermediate scale, models of independent dyadic junctions have revealed how characteristic whole-myocyte properties of ECC emerge from the ensemble behavior of individual release sites. Incorporation of such Ca^{2+} release sites into whole-cell models elucidates the bidirectional interaction between ECC and membrane potential that determine properties of the cardiac AP. Incorporation of ECC regulatory signaling pathways into models has further refined our understanding of this integrative system (see accompanying article in this series by Yang and Saucerman). At the highest scale, such models can be used as building blocks for large scale tissue and whole heart models which can reveal how wave propagation in a normal heart tissue can degenerate into an arrhythmia as a result of defective ECC (see accompanying articles in this series by Weiss et al and Trayanova et al). The continuum of biological scales spanned by these models leads to the formation of powerful multi-scale approaches whereby macroscopic phenotypes (e.g. steep ECC gain curve) can be understood as resulting from microscopic mechanisms (e.g. Ca^{2+} funneling by RyR protein geometry). In the same way that Hodgkin and Huxley formed a mathematical framework that now defines the way in which we conceptualize ion channel function, modern multi-scale models of cardiac ECC have provided a framework for understanding complex ECC mechanisms, interpreting experimental data, and making mechanistic predictions that guide experimental design.

Acknowledgments

Sources of Funding

This work was supported by NIH grants HL081427 and HL087345.

Non-standard Abbreviations and Acronyms

AP	action potential
APD	action potential duration
CaM	calmodulin
CaMKII	Ca^{2+}/calmodulin-dependent protein kinase II
CaN	calcineurin
CaRU	Ca^{2+} release unit
CDI	Ca^{2+}-dependent inactivation
CICR	Ca^{2+}-induced Ca^{2+} release
ClCh	Ca^{2+}-dependent Cl^{-} channel
EAD	early after depolarization
ECC	excitation-contraction coupling
FPE	Fokker-Plank equation
JSR	junctional sarcoplasmic reticulum
LCC	L-type Ca^{2+} channel
LRII	Luo-Rudy phase II
NCX	Na^{+}-Ca^{2+} exchanger
NSR	network sarcoplasmic reticulum
ODE	ordinary differential equation
PKA	protein kinase A
PLB	phospholamban
RyR	ryanodine receptor
SERCA pump	SR Ca^{2+} ATPase
SR	sarcoplasmic reticulum
T-SR	t-tubule/sarcoplasmic reticulum
VDI	voltage-dependent inactivation

References

1. Bers, DM. Excitation-Contraction Coupling and Cardiac Contractile Force. Boston: Kluwer; 2001.
2. Bers DM. Calcium cycling and signaling in cardiac myocytes. Annu Rev Physiol. 2008; 70:23–49. [PubMed: 17988210]
3. Balaban RS, Heineman FW. Control of mitochondrial respiration in the heart in vivo. Mol Cell Biochem. 1989; 89:191–197. [PubMed: 2811864]
4. Williams RS, Rosenberg P. Calcium-dependent gene regulation in myocyte hypertrophy and remodeling. Cold Spring Harb Symp Quant Biol. 2002; 67:339–344. [PubMed: 12858558]
5. Crow MT, Mani K, Nam YJ, Kitsis RN. The mitochondrial death pathway and cardiac myocyte apoptosis. Circ Res. 2004; 95:957–970. [PubMed: 15539639]
6. Brette F, Orchard C. T-tubule function in mammalian cardiac myocytes. Circ Res. 2003; 92:1182–1192. [PubMed: 12805236]

7. Soeller C, Cannell MB. Examinationof the transverse tubular system in living cardiac rat myocytes by 2-photon microscopy and digital image-processing techniques. Circ Res. 1999; 84:266–275. [PubMed: 10024300]
8. Franzini-Armstrong C, Protasi F, Ramesh V. Shape, size, and distribution of Ca(2+) release units and couplons in skeletal and cardiac muscles. Biophys J. 1999; 77:1528–1539. [PubMed: 10465763]
9. Franzini-Armstrong C, Protasi F. Ryanodine receptors of striated muscles: a complex channel capable of multiple interactions. Physiol Rev. 1997; 77:699–729. [PubMed: 9234963]
10. Hayashi T, Martone ME, Yu Z, Thor A, Doi M, Holst MJ, Ellisman MH, Hoshijima M. Three-dimensional electron microscopy reveals new details of membrane systems for Ca2+ signaling in the heart. J Cell Sci. 2009; 122:1005–1013. [PubMed: 19295127]
11. Baddeley D, Jayasinghe ID, Lam L, Rossberger S, Cannell MB, Soeller C. Optical single-channel resolution imaging of the ryanodine receptor distribution in rat cardiac myocytes. Proc Natl Acad Sci U S A. 2009; 106:22275–22280. [PubMed: 20018773]
12. Bers D, Stiffel V. Ratio of ryanodine to dihidropyridine receptors in cardiac and skeletal muscle and implications for E-C coupling. Am J Physiol. 1993; 264:C1587–C1593. [PubMed: 8333507]
13. Fabiato A. Time and calcium dependence of activation and inactivation of calcium-induced release of calcium from the sarcoplasmic reticulum of a skinned canine cardiac Purkinje cell. J Gen Physiol. 1985; 85:247–289. [PubMed: 2580043]
14. Reeves JP, Hale CC. The stoichiometry of the cardiac sodium-calcium exchange system. J Biol Chem. 1984; 259:7733–7739. [PubMed: 6736024]
15. Bers DM, Ginsburg KS. Na:Ca stoichiometry and cytosolic Ca-dependent activation of NCX in intact cardiomyocytes. Ann N Y Acad Sci. 2007; 1099:326–338. [PubMed: 17303827]
16. Philipson KD, Nicoll DA. Sodium-calcium exchange: a molecular perspective. Annu Rev Physiol. 2000; 62:111–133. [PubMed: 10845086]
17. Armoundas AA, Hobai IA, Tomaselli GF, Winslow RL, O'Rourke B. Role of sodium-calcium exchanger in modulating the action potential of ventricular myocytes from normal and failing hearts. Circ Res. 2003; 93:46–53. [PubMed: 12805237]
18. Weber CR, Piacentino V 3rd, Ginsburg KS, Houser SR, Bers DM. Na(+)-Ca(2+) exchange current and submembrane[Ca(2+)] during the cardiac action potential. Circ Res. 2002; 90:182–189. [PubMed: 11834711]
19. Bassani RA, Bassani JW, Bers DM. Mitochondrial and sarcolemmal Ca2+ transport reduce [Ca2+]i during caffeine contractures in rabbit cardiac myocytes. J Physiol. 1992; 453:591–608. [PubMed: 1464847]
20. Hicks MJ, Shigekawa M, Katz AM. Mechanism by which cyclic adenosine 3′:5′-monophosphate-dependent protein kinase stimulates calcium transport in cardiac sarcoplasmic reticulum. Circ Res. 1979; 44:384–391. [PubMed: 216505]
21. Cheng H, Lederer WJ, Cannell MB. Calcium sparks: elementary events underlying excitation-contraction coupling in heart muscle. Science. 1993; 262:740–744. [PubMed: 8235594]
22. Lopez-Lopez JR, Shacklock PS, Balke CW, Wier WG. Local stochastic release of Ca^{2+} in voltage-clamped rat heart cells: visualization with confocal microscopy. J Physiol (Lond). 1994; 480:21–29. [PubMed: 7853223]
23. Soeller C, Cannell MB. Analysing cardiac excitation-contraction coupling with mathematical models of local control. Prog Biophys Mol Biol. 2004; 85:141–162. [PubMed: 15142741]
24. Song LS, Wang SQ, Xiao RP, Spurgeon H, Lakatta EG, Cheng H. beta-Adrenergic stimulation synchronizes intracellular Ca(2+) release during excitation-contraction coupling in cardiac myocytes. Circ Res. 2001; 88:794–801. [PubMed: 11325871]
25. Wier WG, Egan TM, Lopez-Lopez JR, Balke CW. Local control of excitation-contraction coupling in rat heart cells. J Physiol. 1994; 474:463–471. [PubMed: 8014907]
26. Cannell M, Berlin J, Lederer W. Effect of membrane potential changes on the calcium transient in single rat cardiac muscle cells. Science. 1987; 283:1419–1423. [PubMed: 2446391]
27. Stern MD. Theory of excitation-contraction coupling in cardiac muscle. Biophys J. 1992; 63:497–517. [PubMed: 1330031]

28. DiFrancesco D, Noble D. A model of cardiac electrical activity incorporating ionic pumps and concentration changes. Philos Trans R Soc Lond B Biol Sci. 1985; 307:353–398. [PubMed: 2578676]
29. Beeler GW, Reuter H. Reconstruction of the action potential of ventricular myocardial fibres. J Physiol. 1977; 268:177–210. [PubMed: 874889]
30. McAllister RE, Noble D, Tsien RW. Reconstruction of the electrical activity of cardiac Purkinje fibres. J Physiol. 1975; 251:1–59. [PubMed: 1185607]
31. Jafri MS, Rice JJ, Winslow RL. Cardiac Ca2+ dynamics: the roles of ryanodine receptor adaptation and sarcoplasmic reticulum load. Biophys J. 1998; 74:1149–1168. [PubMed: 9512016]
32. Imredy JP, Yue DT. Mechanism of Ca(2+)-sensitive inactivation of L-type Ca2+ channels. Neuron. 1994; 12:1301–1318. [PubMed: 8011340]
33. Stern MD, Song LS, Cheng H, Sham JS, Yang HT, Boheler KR, Rios E. Local control models of cardiac excitation-contraction coupling. A possible role for allosteric interactions between ryanodine receptors. J Gen Physiol. 1999; 113:469–489. [PubMed: 10051521]
34. Greenstein JL, Winslow RL. An integrative model of the cardiac ventricular myocyte incorporating local control of Ca2+ release. Biophys J. 2002; 83:2918–2945. [PubMed: 12496068]
35. Mahajan A, Shiferaw Y, Sato D, Baher A, Olcese R, Xie LH, Yang MJ, Chen PS, Restrepo JG, Karma A, Garfinkel A, Qu Z, Weiss JN. A rabbit ventricular action potential model replicating cardiac dynamics at rapid heart rates. Biophys J. 2008; 94:392–410. [PubMed: 18160660]
36. Hashambhoy YL, Winslow RL, Greenstein JL. CaMKII-induced shift in modal gating explains L-type Ca(2+) current facilitation: a modeling study. Biophys J. 2009; 96:1770–1785. [PubMed: 19254537]
37. Williams GS, Smith GD, Sobie EA, Jafri MS. Models of cardiac excitation-contraction coupling in ventricular myocytes. Math Biosci. 2010; 226:1–15. [PubMed: 20346962]
38. Winslow RL, Rice J, Jafri S, Marban E, O'Rourke B. Mechanisms of altered excitation-contraction coupling in canine tachycardia-induced heart failure, II: model studies. Circ Res. 1999; 84:571–586. [PubMed: 10082479]
39. O'Rourke B, Kass DA, Tomaselli GF, Kaab S, Tunin R, Marban E. Mechanisms of altered excitation-contraction coupling in canine tachycardia-induced heart failure, I: experimental studies. Circ Res. 1999; 84:562–570. [PubMed: 10082478]
40. Ahmmed GU, Dong PH, Song G, Ball NA, Xu Y, Walsh RA, Chiamvimonvat N. Changes in Ca(2+) cycling proteins underlie cardiac action potential prolongation in a pressure-overloaded guinea pig model with cardiac hypertrophy and failure. Circ Res. 2000; 86:558–570. [PubMed: 10720418]
41. Alseikhan BA, DeMaria CD, Colecraft HM, Yue DT. Engineered calmodulins reveal the unexpected eminence of Ca2+ channel inactivation in controlling heart excitation. Proc Natl Acad Sci U S A. 2002; 99:17185–17190. [PubMed: 12486220]
42. Winslow RL, Scollan DF, Holmes A, Yung CK, Zhang J, Jafri MS. Electrophysiological modeling of cardiac ventricular function: from cell to organ. Annu Rev Biomed Eng. 2000; 2:119–155. [PubMed: 11701509]
43. Hund TJ, Rudy Y. Rate dependence and regulation of action potential and calcium transient in a canine cardiac ventricular cell model. Circulation. 2004; 110:3168–3174. [PubMed: 15505083]
44. Luo CH, Rudy Y. A dynamic model of the cardiac ventricular action potential. I. Simulations of ionic currents and concentration changes. Circ Res. 1994; 74:1071–1096. [PubMed: 7514509]
45. Sipido KR, Callewaert G, Carmeliet E. Inhibition and rapid recovery of Ca2+ current during Ca2+ release from sarcoplasmic reticulum in guinea pig ventricular myocytes. Circ Res. 1995; 76:102–109. [PubMed: 8001267]
46. Linz KW, Meyer R. Control of L-type calcium current during the action potential of guinea-pig ventricular myocytes. J Physiol. 1998; 513 (Pt 2):425–442. [PubMed: 9806993]
47. Peterson BZ, DeMaria CD, Adelman JP, Yue DT. Calmodulin is the Ca2+ sensor for Ca2+-dependent inactivation of L-type calcium channels. Neuron. 1999; 22:549–558. [PubMed: 10197534]

48. Rovetti R, Cui X, Garfinkel A, Weiss JN, Qu Z. Spark-induced sparks as a mechanism of intracellular calcium alternans in cardiac myocytes. Circ Res. 2010; 106:1582–1591. [PubMed: 20378857]
49. Langer GA, Peskoff A. Calcium concentration and movement in the diadic cleft space of the cardiac ventricular cell. Biophys J. 1996; 70:1169–1182. [PubMed: 8785276]
50. Soeller C, Cannell MB. Numerical simulation of local calcium movements during L-type calcium channel gating in the cardiac diad. Biophys J. 1997; 73:97–111. [PubMed: 9199775]
51. Cheng H, Lederer WJ. Calcium sparks. Physiol Rev. 2008; 88:1491–1545. [PubMed: 18923188]
52. Sham JS, Song LS, Chen Y, Deng LH, Stern MD, Lakatta EG, Cheng H. Termination of Ca2+ release by a local inactivation of ryanodine receptors in cardiac myocytes. Proc Natl Acad Sci U S A. 1998; 95:15096–15101. [PubMed: 9844021]
53. Gyorke I, Hester N, Jones LR, Gyorke S. The role of calsequestrin, triadin, and junctin in conferring cardiac ryanodine receptor responsiveness to luminal calcium. Biophys J. 2004; 86:2121–2128. [PubMed: 15041652]
54. Shannon TR, Wang F, Puglisi J, Weber C, Bers DM. A mathematical treatment of integrated Ca dynamics within the ventricular myocyte. Biophys J. 2004; 87:3351–3371. [PubMed: 15347581]
55. Hashambhoy YL, Greenstein JL, Winslow RL. Role of CaMKII in RyR leak, EC coupling and action potential duration: a computational model. J Mol Cell Cardiol. 2010; 49:617–624. [PubMed: 20655925]
56. Zahradnikova A, Zahradnik I. A minimal gating model for the cardiac calcium release channel. Biophys J. 1996; 71:2996–3012. [PubMed: 8968571]
57. Keizer J, Levine L. Ryanodine receptor adaptation and Ca2+(−)induced Ca2+ release-dependent Ca2+ oscillations. Biophys J. 1996; 71:3477–3487. [PubMed: 8968617]
58. Cheng H, Fill M, Valdivia H, Lederer WJ. Models of Ca2+ release channel adaptation. Science. 1995; 267:2009–2010. [PubMed: 7701326]
59. Gyorke S, Fill M. Ryanodine receptor adaptation: control mechanism of Ca(2+)-induced Ca2+ release in heart. Science. 1993; 260:807–809. [PubMed: 8387229]
60. Rice JJ, Jafri MS, Winslow RL. Modeling gain and gradedness of Ca2+ release in the functional unit of the cardiac diadic space. Biophys J. 1999; 77:1871–1884. [PubMed: 10512809]
61. Grandi E, Pasqualini FS, Bers DM. A novel computational model of the human ventricular action potential and Ca transient. J Mol Cell Cardiol. 2010; 48:112–121. [PubMed: 19835882]
62. Sobie EA, Dilly KW, dos Santos Cruz J, Lederer WJ, Jafri MS. Termination of cardiac Ca(2+) sparks: an investigative mathematical model of calcium-induced calcium release. Biophys J. 2002; 83:59–78. [PubMed: 12080100]
63. Gyorke I, Gyorke S. Regulation of the cardiac ryanodine receptor channel by luminal Ca2+ involves luminal Ca2+ sensing sites. Biophys J. 1998; 75:2801–2810. [PubMed: 9826602]
64. Marx SO, Gaburjakova J, Gaburjakova M, Henrikson C, Ondrias K, Marks AR. Coupled gating between cardiac calcium release channels (ryanodine receptors). Circ Res. 2001; 88:1151–1158. [PubMed: 11397781]
65. Sobie EA, Guatimosim S, Gomez-Viquez L, Song LS, Hartmann H, Saleet Jafri M, Lederer WJ. The Ca 2+ leak paradox and rogue ryanodine receptors: SR Ca 2+ efflux theory and practice. Prog Biophys Mol Biol. 2006; 90:172–185. [PubMed: 16326215]
66. Groff JR, Smith GD. Ryanodine receptor allosteric coupling and the dynamics of calcium sparks. Biophys J. 2008; 95:135–154. [PubMed: 18359795]
67. Shannon TR, Guo T, Bers DM. Ca2+ scraps: local depletions of free [Ca2+] in cardiac sarcoplasmic reticulum during contractions leave substantial Ca2+ reserve. Circ Res. 2003; 93:40–45. [PubMed: 12791706]
68. Zima AV, Picht E, Bers DM, Blatter LA. Termination of cardiac Ca2+ sparks: role of intra-SR [Ca2+], release flux, and intra-SR Ca2+ diffusion. Circ Res. 2008; 103:e105–115. [PubMed: 18787194]
69. Stevens SC, Terentyev D, Kalyanasundaram A, Periasamy M, Gyorke S. Intra-sarcoplasmic reticulum Ca2+ oscillations are driven by dynamic regulation of ryanodine receptor function by luminal Ca2+ in cardiomyocytes. J Physiol. 2009; 587:4863–4872. [PubMed: 19703963]

70. Zima AV, Picht E, Bers DM, Blatter LA. Partial inhibition of sarcoplasmic reticulum ca release evokes long-lasting ca release events in ventricular myocytes: role of luminal ca in termination of ca release. Biophys J. 2008; 94:1867–1879. [PubMed: 18024505]
71. Greenstein JL, Hinch R, Winslow RL. Mechanisms of excitation-contraction coupling in an integrative model of the cardiac ventricular myocyte. Biophys J. 2006; 90:77–91. [PubMed: 16214852]
72. Hinch R, Greenstein JL, Tanskanen AJ, Xu L, Winslow RL. A simplified local control model of calcium-induced calcium release in cardiac ventricular myocytes. Biophys J. 2004; 87:3723–3736. [PubMed: 15465866]
73. Tanskanen AJ, Greenstein JL, Chen A, Sun SX, Winslow RL. Protein geometry and placement in the cardiac dyad influence macroscopic properties of calcium-induced calcium release. Biophys J. 2007; 92:3379–3396. [PubMed: 17325016]
74. Serysheva, Hamilton SL, Chiu W, Ludtke SJ. Structure of Ca2+ release channel at 14 A resolution. J Mol Biol. 2005; 345:427–431. [PubMed: 15581887]
75. Wang MC, Collins RF, Ford RC, Berrow NS, Dolphin AC, Kitmitto A. The three-dimensional structure of the cardiac L-type voltage-gated calcium channel: comparison with the skeletal muscle form reveals a common architectural motif. J Biol Chem. 2004; 279:7159–7168. [PubMed: 14634003]
76. Wilson MA, Brunger AT. the 1.0 A crystal structure of Ca2+-bound calcmodulin: an analysis of disorder and implications for functionally relevant plasticity. J Mol Biol. 2000; 301(5):1237–1256. [PubMed: 10966818]
77. Bhalla US. Signaling in small subcellular volumes. I. Stochastic and diffusion effects on individual pathways. Biophys J. 2004; 87:733–744. [PubMed: 15298882]
78. Wang SQ, Stern MD, Rios E, Cheng H. The quantal nature of Ca2+ sparks and in situ operation of the ryanodine receptor array in cardiac cells. Proc Natl Acad Sci U S A. 2004; 101:3979–3984. [PubMed: 15004280]
79. Rose WC, Balke CW, Wier WG, Marban E. Macroscopic and unitary properties of physiological ion flux through L-type Ca2+ channels in guinea-pig heart cells. J Physiol. 1992; 456:267–284. [PubMed: 1338098]
80. Risken, H. The Fokker-Planck equation. Berlin: Springer; 1997.
81. Wang H, Peskin CS, Elston TC. A robust numerical algorithm for studying biomolecular transport processes. J Theor Biol. 2003:221.
82. Shannon TR, Ginsburg KS, Bers DM. Reverse mode of the sarcoplasmic reticulum calcium pump and load-dependent cytosolic calcium decline in voltage-clamped cardiac ventricular myocytes. Biophys J. 2000; 78:322–333. [PubMed: 10620296]
83. Wang SQ, Song LS, Lakatta EG, Cheng H. Ca2+ signalling between single L-type Ca2+ channels and ryanodine receptors in heart cells. Nature. 2001; 410:592–596. [PubMed: 11279498]
84. Hobai IA, O'Rourke B. Decreased sarcoplasmic reticulum calcium content is responsible for defective excitation-contraction coupling incanine heart failure. Circulation. 2001; 103:1577–1584. [PubMed: 11257088]
85. Keizer J, Smith GD. Spark-to-wave transition: saltatory transmission of calcium waves in cardiac myocytes. Biophys Chem. 1998; 72:87–100. [PubMed: 9652087]
86. Collier ML, Levesque PC, Kenyon JL, Hume JR. Unitary Cl-channels activated by cytoplasmic Ca2+ in canine ventricular myocytes. Circ Res. 1996; 78:936–944. [PubMed: 8620614]
87. Tanskanen AJ, Greenstein JL, O'Rourke B, Winslow RL. The role of stochastic and modal gating of cardiac L-type Ca2+ channels on early after-depolarizations. Biophys J. 2005; 88:85–95. [PubMed: 15501946]
88. Santana LF, Cheng H, Gomez AM, Cannell MB, Lederer WJ. Relation between the sarcolemmal Ca2+ current and Ca2+ sparks and local control theories for cardiac excitation-contraction coupling. Circ Res. 1996; 78:166–171. [PubMed: 8603501]
89. Williams GS, Huertas MA, Sobie EA, Jafri MS, Smith GD. A probability density approach to modeling local control of calcium-induced calcium release in cardiac myocytes. Biophys J. 2007; 92:2311–2328. [PubMed: 17237200]

90. Williams GS, Huertas MA, Sobie EA, Jafri MS, Smith GD. Momentclosure for local control models of calcium-induced calcium release in cardiac myocytes. Biophys J. 2008; 95:1689–1703. [PubMed: 18487291]
91. Flaim SN, Giles WR, McCulloch AD. Contributions of sustained INa and IKv43 to transmural heterogeneity of early repolarization and arrhythmogenesis in canine left ventricular myocytes. Am J Physiol Heart Circ Physiol. 2006; 291:H2617–2629. [PubMed: 16829642]
92. Livshitz L, Rudy Y. Uniqueness and stability of action potential models during rest, pacing, and conduction using problem-solving environment. Biophys J. 2009; 97:1265–1276. [PubMed: 19720014]
93. Saucerman JJ, Bers DM. Calmodulin mediates differential sensitivity of CaMKII and calcineurin to local Ca2+ in cardiac myocytes. Biophys J. 2008; 95:4597–4612. [PubMed: 18689454]
94. Bers DM. Cardiac excitation-contraction coupling. Nature. 2002; 415:198–205. [PubMed: 11805843]
95. Pasek M, Simurda J, Orchard CH, Christe G. A model of the guinea-pig ventricular cardiac myocyte incorporating a transverse-axial tubular system. Prog Biophys Mol Biol. 2008; 96:258–280. [PubMed: 17888503]
96. Goldhaber JI, Lamp ST, Walter DO, Garfinkel A, Fukumoto GH, Weiss JN. Local regulation of the threshold for calcium sparks in rat ventricular myocytes: role of sodium-calcium exchange. J Physiol. 1999; 520(Pt 2):431–438. [PubMed: 10523412]
97. Litwin S, Kohmoto O, Levi AJ, Spitzer KW, Bridge JH. Evidence that reverse Na-Ca exchange can trigger SR calcium release. Ann N Y Acad Sci. 1996; 779:451–463. [PubMed: 8659861]
98. Lewartowski B, Janiak R, Langer GA. Effect of sarcoplasmic reticulum Ca release into diadic region on Na/Ca exchange in cardiac myocytes. J Physiol Pharmacol. 1996; 47:577–590. [PubMed: 9116325]
99. Thomas MJ, Sjaastad I, Andersen K, Helm PJ, Wasserstrom JA, Sejersted OM, Ottersen OP. Localization and function of the Na+/Ca2+-exchanger in normal and detubulated rat cardiomyocytes. J Mol Cell Cardiol. 2003; 35:1325–1337. [PubMed: 14596789]
100. Mohler PJ, Davis JQ, Bennett V. Ankyrin-B coordinates the Na/K ATPase, Na/Ca exchanger, and InsP3 receptor in a cardiac T-tubule/SR microdomain. PLoS Biol. 2005; 3:e423. [PubMed: 16292983]
101. Lines GT, Sande JB, Louch WE, Mork HK, Grottum P, Sejersted OM. Contribution of the Na+/Ca2+ exchanger to rapid Ca2+ release in cardiomyocytes. Biophys J. 2006; 91:779–792. [PubMed: 16679359]
102. Bossuyt J, Ai X, Moorman JR, Pogwizd SM, Bers DM. Expression and phosphorylation of the na-pump regulatory subunit phospholemman in heart failure. Circ Res. 2005; 97:558–565. [PubMed: 16100047]
103. Rizzuto R, Duchen MR, Pozzan T. Flirting in little space: the ER/mitochondria Ca2+ liaison. Sci STKE. 2004; 2004:re1. [PubMed: 14722345]
104. Sharma VK, Ramesh V, Franzini-Armstrong C, Sheu SS. Transport of Ca2+ from sarcoplasmic reticulum to mitochondria in rat ventricular myocytes. J Bioenerg Biomembr. 2000; 32:97–104. [PubMed: 11768767]
105. Kirichok Y, Krapivinsky G, Clapham DE. The mitochondrial calcium uniporter is a highly selective ion channel. Nature. 2004; 427:360–364. [PubMed: 14737170]
106. Maack C, O'Rourke B. Excitation-contraction coupling and mitochondrial energetics. Basic Res Cardiol. 2007; 102:369–392. [PubMed: 17657400]
107. Greenstein JL, Tanskanen AJ, Winslow RL. Modeling the actions of beta-adrenergic signaling on excitation--contraction coupling processes. Ann N Y Acad Sci. 2004; 1015:16–27. [PubMed: 15201146]
108. Saucerman JJ, Brunton LL, Michailova AP, McCulloch AD. Modeling beta-adrenergic control of cardiac myocyte contractility in silico. J Biol Chem. 2003; 278:47997–48003. [PubMed: 12972422]
109. Puglisi JL, Bers DM. LabHEART: an interactive computer model of rabbit ventricular myocyte ion channels and Ca transport. Am J Physiol Cell Physiol. 2001; 281:C2049–2060. [PubMed: 11698264]

110. Faber GM, Rudy Y. Action potential and contractility changes in [Na(+)](i) overloaded cardiac myocytes: a simulation study. Biophys J. 2000; 78:2392–2404. [PubMed: 10777735]

111. Ahrens-Nicklas RC, Clancy CE, Christini DJ. Re-evaluating the efficacy of β-adrenergic agonists and antagonists in long QT-3 syndrome through computational modelling. Cardiovascular Research. 2009; 82:439–447. [PubMed: 19264765]

112. Maier LS, Bers DM. Role of Ca2+/calmodulin-dependent protein kinase (CaMK) in excitation-contraction coupling in the heart. Cardiovasc Res. 2007; 73:631–640. [PubMed: 17157285]

113. Currie S, Loughrey CM, Craig MA, Smith GL. Calcium/calmodulin-dependent protein kinase IIdelta associates with the ryanodine receptor complex and regulates channel function in rabbit heart. Biochem J. 2004; 377:357–366. [PubMed: 14556649]

114. Hudmon A, Schulman H, Kim J, Maltez JM, Tsien RW, Pitt GS. CaMKII tethers to L-type Ca2+ channels, establishing a local and dedicated integrator of Ca2+ signals for facilitation. J Cell Biol. 2005; 171:537–547. [PubMed: 16275756]

115. Ai X, Curran JW, Shannon TR, Bers DM, Pogwizd SM. Ca2+/calmodulin-dependent protein kinase modulates cardiac ryanodine receptor phosphorylation and sarcoplasmic reticulum Ca2+ leak in heart failure. Circ Res. 2005; 97:1314–1322. [PubMed: 16269653]

116. Grandi E, Puglisi JL, Wagner S, Maier LS, Severi S, Bers DM. Simulation of Ca-calmodulin-dependent protein kinase II on rabbit ventricular myocyte ion currents and action potentials. Biophys J. 2007; 93:3835–3847. [PubMed: 17704163]

117. Tadross MR, Dick IE, Yue DT. Mechanism of local and global Ca2+ sensing by calmodulin in complex with a Ca2+ channel. Cell. 2008; 133:1228–1240. [PubMed: 18585356]

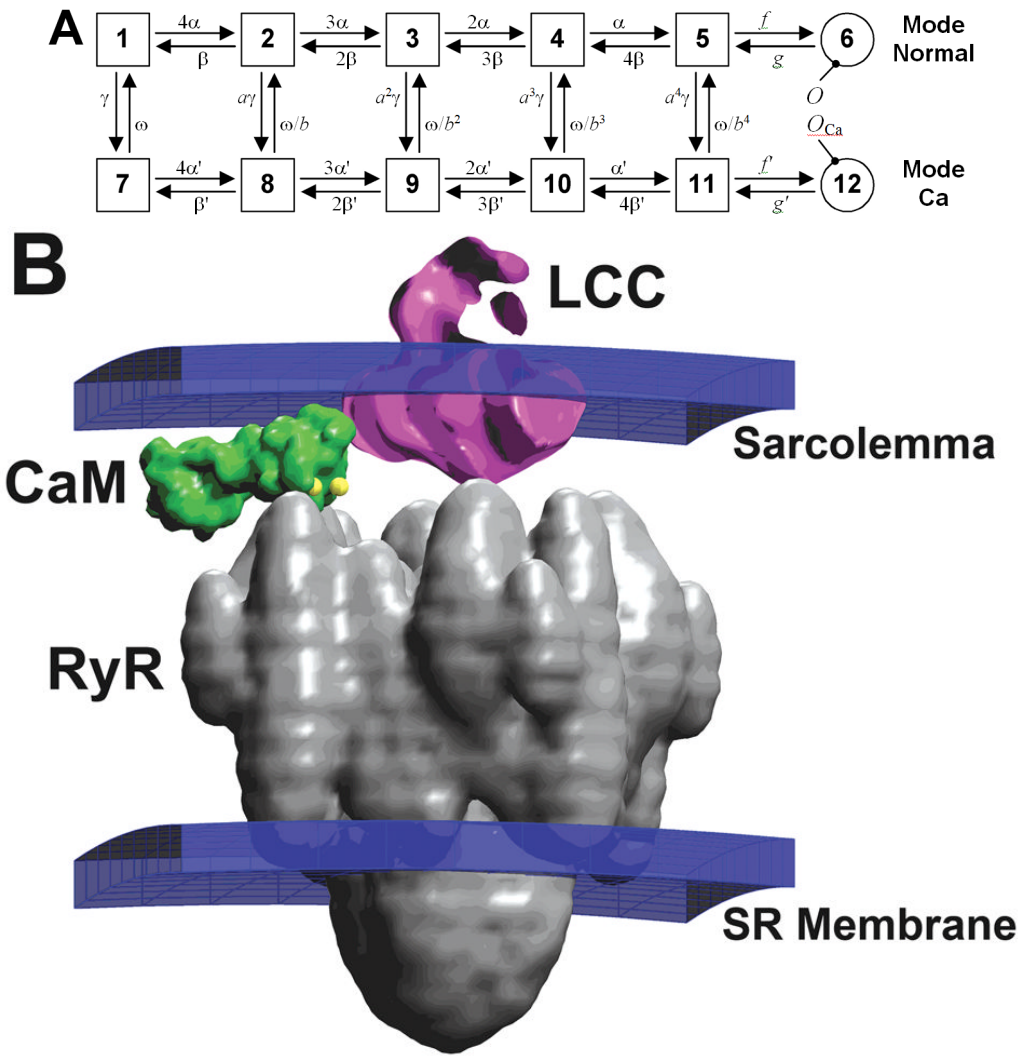

Figure 1.

(A) Markov state model for gating of the LCC as proposed by Jafri et al.[31] CDI occurs as a result of downward transitions from model-normal to mode-Ca. VDI is described by an independent Hodgkin-Huxley type gate (not shown). (B) Structure of a region of the dyad containing one LCC opposed to a single RyR, and one CaM molecule tethered to the LCC[73].

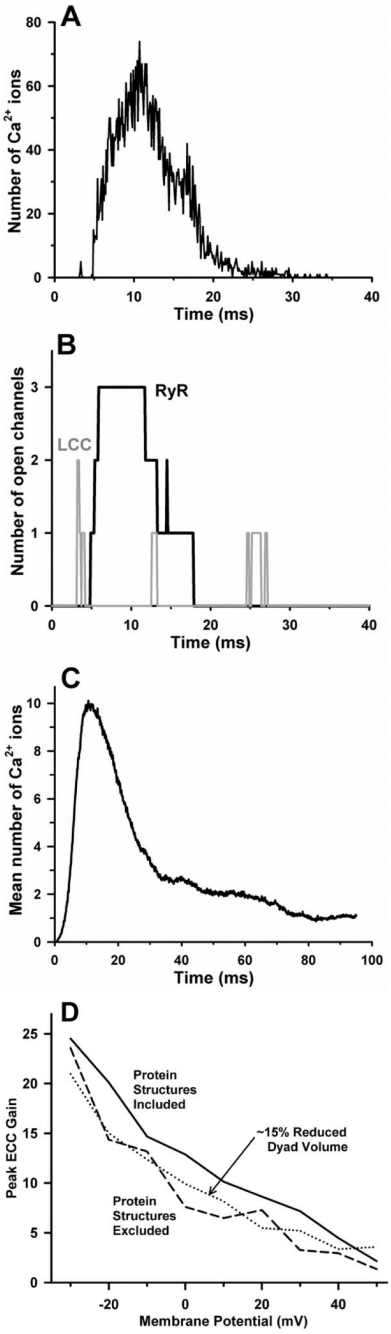

Figure 2.

A CICR event in a single dyad evoked by a 0 mV voltage clamp step at time zero (from[73]). (A) The number of free Ca^{2+} ions in the dyad volume as a function of time. (B) The number of open RyRs (black solid line) and the number of open LCCs (gray solid line) in the dyad during the release event depicted in panel A. (C) The average number of free Ca^{2+} ions in the dyad as calculated from 400 independent dyads. (D) ECC gain as a function of membrane potential for the baseline model which includes space-filling geometric models of protein structure in the dyad (solid line), for the model with protein structures excluded (dashed line), and for a modified model with dyad height reduced from 15 nm to 13 nm and protein structures excluded (dotted line).

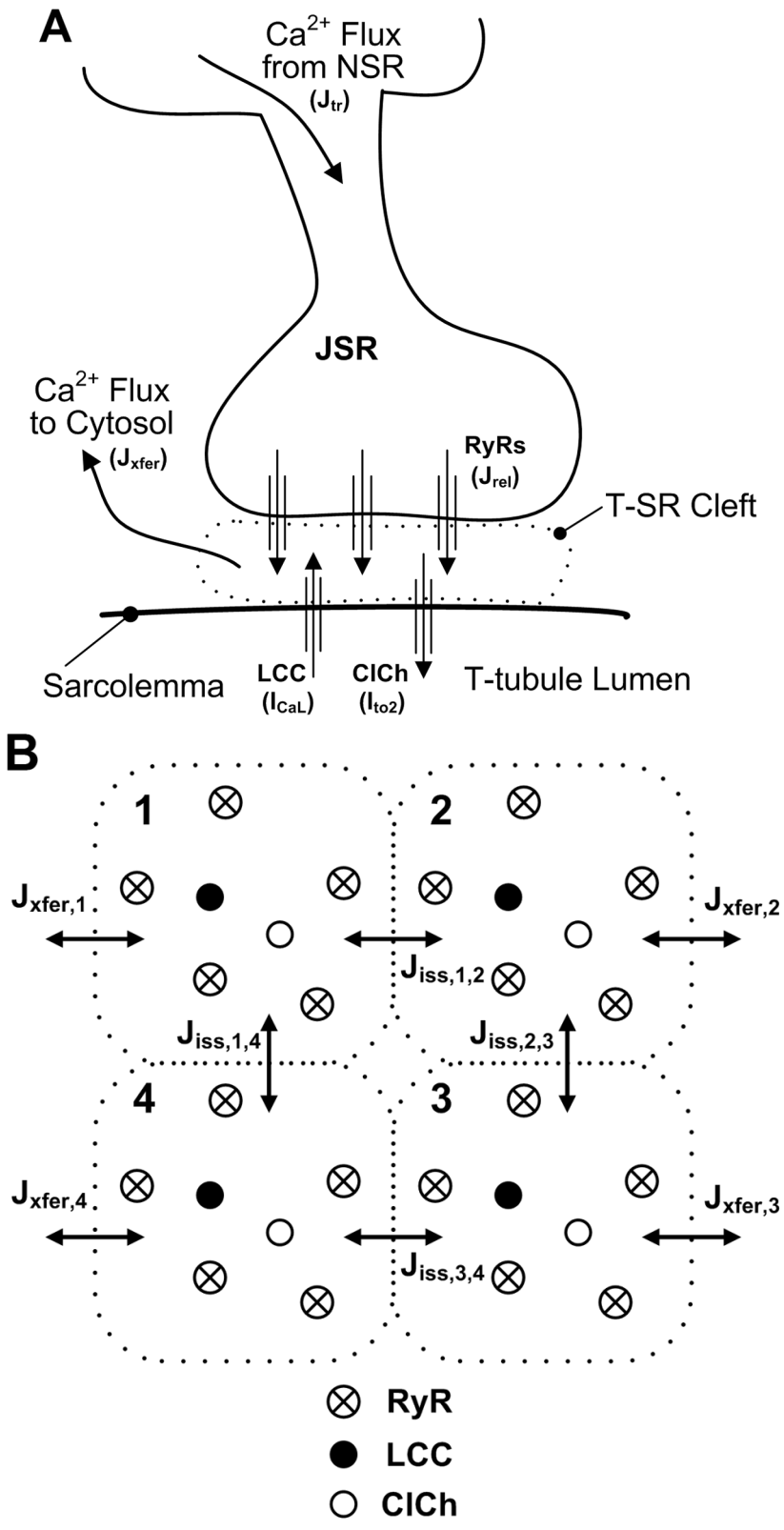

Figure 3.

Schematic representation of the CaRU[34]. (A) Trigger Ca^{2+} influx through the LCCs enters into the T-SR cleft (dyadic space), RyRs and ClChs open, local Ca^{2+} passively diffuses into the cytosol, and JSR Ca^{2+} is refilled via passive diffusion from the NSR. (B) The T-SR cleft (shown in cross-section) is composed of four dyadic subspace volumes, arranged on a 2 × 2 grid, each containing 1 LCC, 1 ClCh, and 5 RyRs. Ca^{2+} in any subspace may diffuse to a neighboring subspace (J_{iss}) or to the cytosol (J_{xfer}).

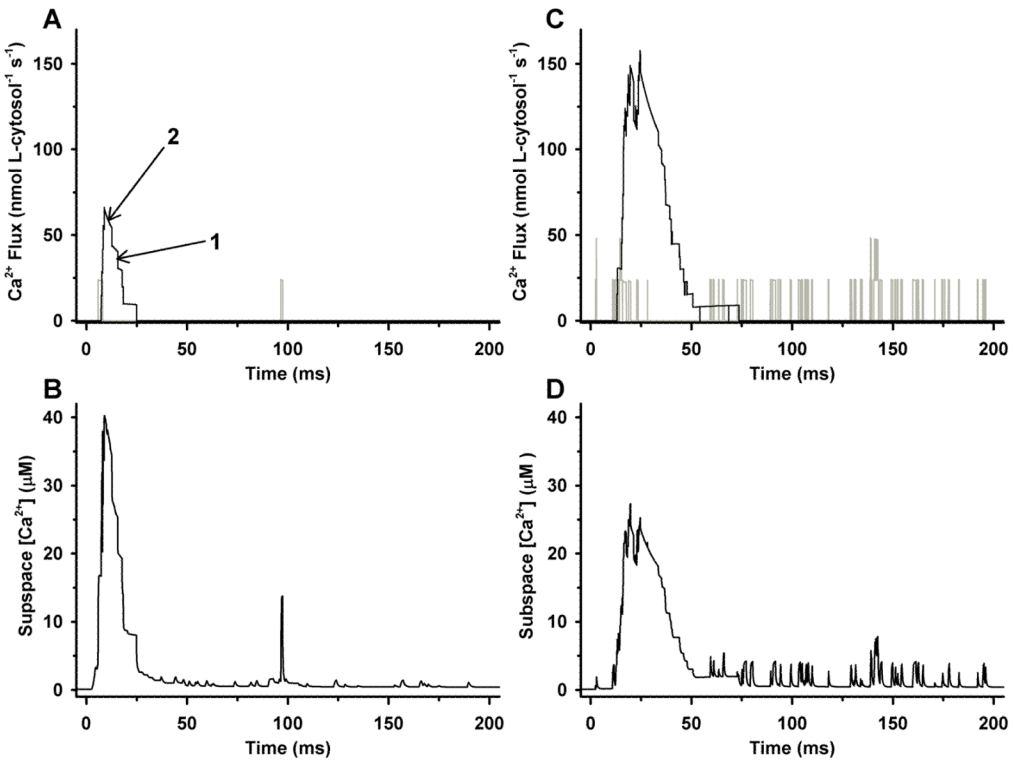

Figure 4.

Sample results for a single CaRU in response to a 200-ms voltage clamp to 0 mV[34]. (A) Ca^{2+} flux through a single LCC (gray line) and through the set of five RyRs (black line) within a single dyadic subspace compartment. Arrows 1 and 2 highlight RyR number and Ca^{2+} gradient driven changes in SR Ca^{2+} release flux, respectively. (B) Subspace [Ca^{2+}] associated with the events of panel A. (C) Ca^{2+} flux through the set of four LCCs (gray line) and the set of 20 RyRs (black line) within a single CaRU. (D). Mean subspace [Ca^{2+}] in the four subspace compartments associated with the events in the CaRU described in panel C.

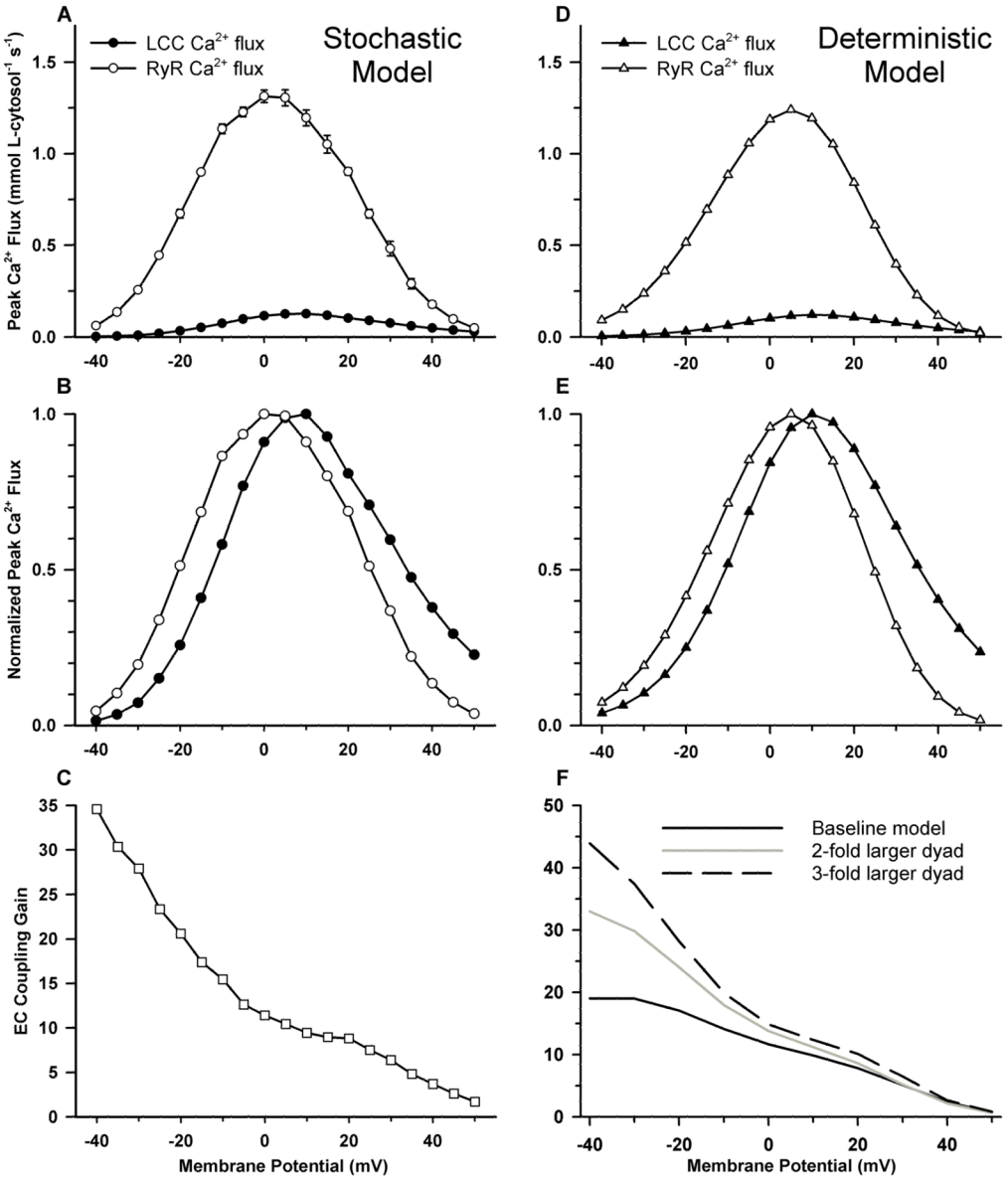

Figure 5.

Ca^{2+} fluxes and ECC gain for the Greenstein-Winslow model (panels A-C)[34] and coupled LCC-RyR model (panels D-F)[71]. (A) Mean peak LCC (filled circles) and RyR (open circles) Ca^{2+} flux amplitudes as a function of membrane voltage. (B) Normalized peak Ca^{2+} fluxes (data of panel A). (C) ECC gain under control conditions. (D) Peak LCC (filled triangles) and RyR (open triangles) Ca^{2+} flux amplitudes. (E) Normalized peak Ca^{2+} fluxes (data of panel D). (F) ECC gain for the baseline model (solid line), and models in which dyad size and number of channels per dyad is increased twofold (gray line), and threefold (dashed line).

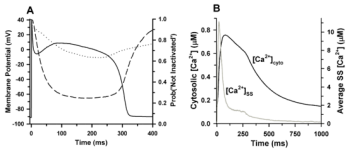

Figure 6.

AP and Ca^{2+} transients at 1-Hz steady state pacing[34]. (A) Membrane potential (solid line, left axis), and probability that CDI and VDI (dashed and dotted lines, respectively, right axis) has not occurred as a function of time under normal conditions. (B) Cytosolic (black line, left axis) and mean subspace (gray line, right axis) Ca^{2+} concentrations corresponding to the AP simulated in panel A.

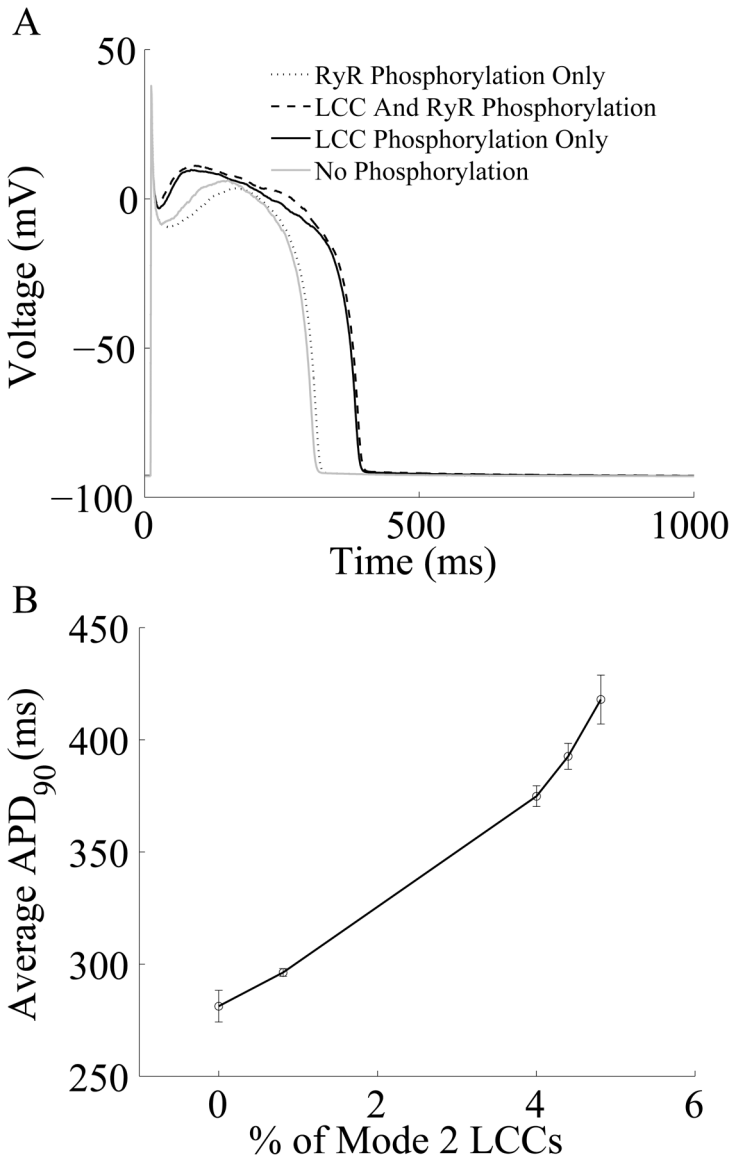

Figure 7.
(A) Simulated Results from a 1-Hz AP pacing protocol under different LCC and/or RyR phosphorylation conditions. (B) APD as a function of average LCC phosphorylation levels. Fully phosphorylated LCCs gate in Mode 2 which exhibit long duration openings.[55]